Journal of Nanophotonics

Nanophotonics.SPIEDigitalLibrary.org

Modeling and optimization of Au-GaAs plasmonic nanoslit array structures for enhanced near-infrared photodetector applications

Zachary T. Brawley
Stephen J. Bauman
Grant P. Abbey
Ahmad A. Darweesh
Ahmad I. Nusir
Omar Manasreh
Joseph B. Herzog

SPIE.

Zachary T. Brawley, Stephen J. Bauman, Grant P. Abbey, Ahmad A. Darweesh, Ahmad I. Nusir, Omar Manasreh, Joseph B. Herzog, "Modeling and optimization of Au-GaAs plasmonic nanoslit array structures for enhanced near-infrared photodetector applications," *J. Nanophoton.* **11**(1), 016017 (2017), doi: 10.1117/1.JNP.11.016017.

Modeling and optimization of Au-GaAs plasmonic nanoslit array structures for enhanced near-infrared photodetector applications

Zachary T. Brawley,[a,b] Stephen J. Bauman,[c] Grant P. Abbey,[a,c] Ahmad A. Darweesh,[c] Ahmad I. Nusir,[d] Omar Manasreh,[d] and Joseph B. Herzog[a,c,*]

[a]University of Arkansas, Department of Physics, Fayetteville, Arkansas, United States
[b]University of Central Arkansas, Department of Physics and Astronomy, Conway, Arkansas, United States
[c]University of Arkansas, Microelectronics-Photonics Graduate Program, Fayetteville, Arkansas, United States
[d]University of Arkansas, Department of Electrical Engineering, Fayetteville, Arkansas, United States

Abstract. This theoretical work explores how various geometries of Au plasmonic nanoslit array structures improve the total optical enhancement in GaAs photodetectors. Computational models studied these characteristics. Varying the electrode spacing, width, and thickness drastically affected the enhancement in the GaAs. Peaks in enhancement decayed as Au widths and thicknesses increased. These peaks are resonant with the incident near-infrared wavelength. The enhancement values were found to increase with decreasing electrode spacing. Additionally, a calculation was conducted for a model containing Ti between the Au and the GaAs to simulate the necessary adhesion layer. It was found that optical enhancement in the GaAs decreases for increasing Ti layer thickness. Optimal dimensions for the Au electrode include a width of 240 nm, thickness of 60 nm, electrode spacing of 5 nm, and a minimum Ti thickness. Optimal design has been shown to improve enhancement to values that are up to 25 times larger than for nonoptimized geometries and up to 300 times over structures with large electrode spacing. It was also found that the width of the metal in the array plays a more significant role in affecting the field enhancement than does the period of the array. [DOI: 10.1117/1.JNP.11.016017]

Keywords: plasmonic; nanoslit array; nano-optics; photodetector; grating; enhancement.

Paper 16179P received Nov. 17, 2016; accepted for publication Mar. 13, 2017; published online Mar. 23, 2017.

1 Introduction

Light incident on a metallic surface causes the conduction electrons of the solid to oscillate at a characteristic frequency dependent on the radiation energy and the material properties. The quantized, collective oscillations of free electrons in a metal are known as surface plasmons, and they exhibit their own enhanced local electromagnetic fields, which may be harnessed for applications that benefit from the strengthening of electromagnetic field intensity.[1] The electromagnetic intensity in the near-field region next to plasmonic structures can be many times that of the incident radiation, making plasmonic structures useful for optical signal enhancement. Plasmonic devices can be tuned to improve sensing and photovoltaic devices. This has led to much research in determining optimal device parameters that will generate the maximum enhancement. Common geometries include nanowire and nanotoroid arrays as these structures can be accurately modeled and fabricated.[2,3]

*Address all correspondence to: Joseph B. Herzog, E-mail: jbherzog@uark.edu

This work investigates nanoscale geometries that have not been studied before in plasmonic nanoslit array structures on photodetectors. The effects of each parameter on the local field enhancement are also studied with the goal of maximizing enhancement in optoelectronic devices. The radiated electromagnetic field generated by the surface plasmons in the metal is effectively scattered into the device's active region, the optical near-field if one considers the metallic structure as an antenna. As a result, the nanostructures can produce a net increase in the local electric field E_{loc}, the field at points near the nanostructure. The enhanced light intensity, referred to here as optical enhancement, is defined as the square of the ratio between the local electric field strength E_{loc} and the incident field E_0, $(E_{loc}/E_0)^2$.[1,4] This increased local intensity can improve optical device performance.

A horizontally periodic array of metallic nanostructures separated by dielectric nanogaps on a substrate is called a nanoslit array or sometimes a plasmonic grating.[5–13] Applications of devices containing nanoslit structures include biosensors,[5,14] terahertz antennas,[9] and lenses with controllable parameters.[15–18] Experimental and theoretical research has confirmed that not only can these nanostructures enhance an incident electric field, but also the nanogaps that separate them can provide additional enhancement.[19–22] Field "hotspots" are produced via nanogap structures multiplying the magnitude of the electric field due to the plasmonic coupling between adjacent nanostructures. These hotspots can be harnessed for a variety of different applications, including surface-enhanced Raman spectroscopy,[23] single-molecule detection,[24–27] photovoltaics,[28–35] biosensing,[36–42] and photodetectors.[43,44]

Prior work has investigated plasmonic effects in microscale interdigital electrodes,[45,46] but the current work extends the research to the nanoscale where plasmonic effects are more significant. Additionally, due to a recently demonstrated fabrication technique that can create sub-10 nm gaps,[47] these new geometries, which have not before been studied, are now carefully explored. Various structural parameters are modified to determine the conditions for maximum optical enhancement occurring in the GaAs substrate layer of the model, emphasizing the additional generation of optical enhancement in the device. Analysis of the plasmonic structure geometry will lead to more efficient enhanced photonic devices.[48]

Many metal–semiconductor interfaces need some form of adhesion to ensure that the more desirable plasmonically active metal (typically Au or Ag) stays attached to the surface of the semiconductor. Commonly, thin layers (nanometers) of Ti, Cr, or other metals are used as the adhesive.[49] Nanofabrication techniques usually deposit a semiuniform layer of the adhesion material prior to deposition of the desired metal. Although usually necessary, it has been shown that this layer produces "damping" effects of the plasmonic enhancement that occurs in the near-field of the structure.[49] In the nanomasking process utilized by the Herzog group, a Ti adhesion layer is most commonly used because a sacrificial Cr layer is required for the fabrication process.[47] Thus, the current work studies the effects of varying the thickness of a Ti adhesion layer on the local plasmonic field enhancement.

2 Method

A top view of the representative GaAs photodetector device that has been modeled for this work is shown in Fig. 1(a). The center nanoslit array section, Fig. 1(b), can approximate the plasmonic properties of the entire device. A 2-D cross section of this region, depicted in Fig. 1(c), was modeled in this work; it contains Au nanowires on a GaAs substrate with a Ti adhesion layer, all beneath an air region.

A cross-sectional finite element method (COMSOL Multiphysics) model was created for the Au nanostructures on a substrate surface. Material properties were assigned to the applicable areas of the model,[50,51] geometrical parameters of the structure were variable, and a light wave was simulated as incident downward normal to the substrate surface with an electric field amplitude of E_0. A mesh was created over the entire model space, and a calculation was performed to determine the electric field E_{loc} at each finite mesh element. Once the model was built, many different geometries were analyzed to determine which produced the optimal average optical enhancement; the enhancement $(E_{loc}/E_0)^2$ was calculated at each mesh element and the average of all elements in the GaAs region was used to produce a single, average optical

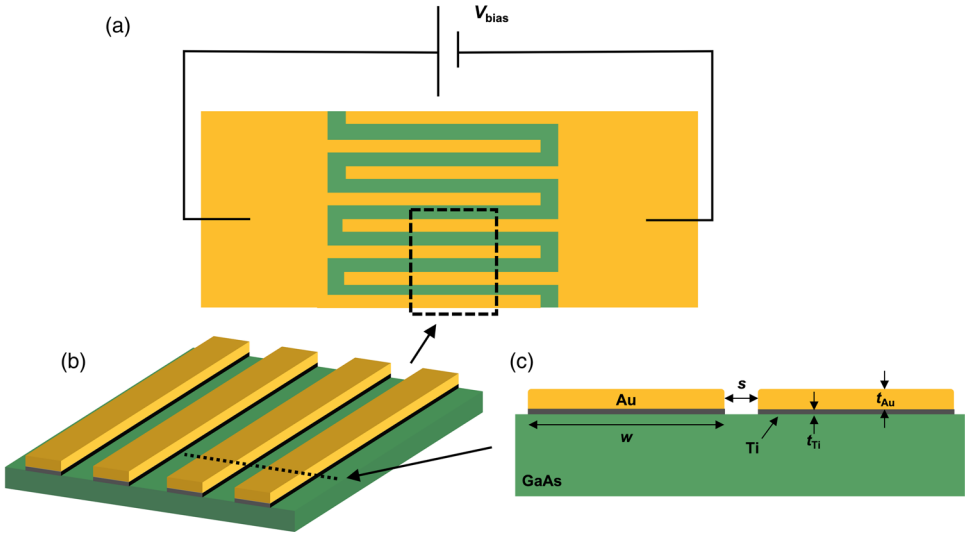

Fig. 1 Schematic drawing of Au nanowires on a GaAs semiconductor substrate bonded by a Ti adhesion layer. (a) Top-view schematic of potential photodetector device with interdigital electrodes, (b) 3-D representation of electrodes as an infinite array, and (c) side view showing the parameters that were swept to find the dimensions for optimal optical enhancement: electrode gap (s), Au width (w), Au thickness (t_{Au}), and Ti thickness (t_{Ti}).

enhancement value. Four parametric sweeps were performed to analyze the effects on the enhancement: varying the Ti thickness, Au width, Au thickness, and electrode spacing.

A light wave of wavelength 875 nm, in tune with the bandgap of GaAs, was simulated as incident from the top of the model and polarized along the electrode width.[52] Fillets (5-nm radius) were applied to the top corners of the nanostructures to more accurately represent the rounded corners of fabricated metallic nanostructures. Periodic boundary conditions were applied to both sides of the simulation space to approximate an infinite horizontal array of interdigitated nanoscale electrodes. The period of the electrodes, and thus the simulation space, is $P = w + s$. Figure 1(c) displays twice the simulation width, $2P$, for visualization purposes. Due to the cross-sectional nature of the model, the wires are also infinite in length.

3 Results and Discussion

First, a numerical analysis was performed to find the average optical enhancement over the entire GaAs layer for various Ti thicknesses. The thickness of the Ti layer was swept from 1 to 10 nm, then totally removed from the model. Increasing the Ti layer was found to not only move the hotspot away from the GaAs but also to reduce the magnitude of the plasmonic resonance caused by the incident light, as shown in Figs. 2(a) and 2(b) and as first studied by Abbey et al.[52]

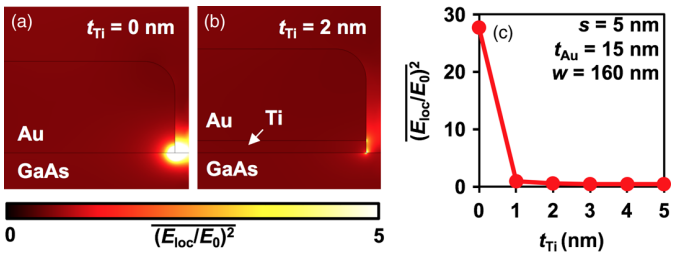

Fig. 2 Effect of Ti layer thickness on optical enhancement in the GaAs. Optical intensity distribution of (a) Au in direct contact with GaAs substrate and (b) Au adhered to GaAs by a Ti layer ($t_{Ti} = 2$ nm). The color bar indicates optical enhancement $(E_{loc}/E_0)^2$. (c) Plot of average optical enhancement within the entire GaAs layer versus t_{Ti}. For (a–c), $s = 5$ nm, $t_{Au} = 15$ nm, and $w = 160$ nm.

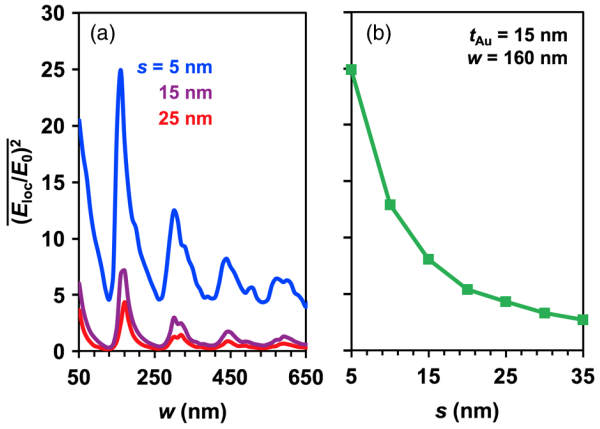

Fig. 3 Optical enhancement in the GaAs as a function of Au width and electrode spacing. (a) Average optical enhancement versus Au width (w) at three electrode spacings ($s = 5$, 15, and 25 nm). The Au thickness was held constant at $t_{Au} = 15$ nm, and there was no Ti layer. (b) Plot of the maximum peak versus s at $w = 160$ nm.

Figure 2(c) is a plot of the normalized enhancement in the GaAs as a function of Ti thickness. Total removal of the Ti resulted in an increase in enhancement of more than 20 times the value for a 1-nm Ti layer. Since Ti has a much larger imaginary dielectric function component than that of gold, it contributes to more plasmonic damping in the nanostructure.[53] Additionally, the hotspot at the edge of the Au structure is moved away from the GaAs layer with increasing Ti layer thickness, decreasing the optical enhancement in the GaAs. Charge interactions between the Ti/Au interfaces can also lead to further plasmonic damping.[53] As the plasmon is damped, the enhancement is decreased.

The average optical enhancement was also studied as a function of Au width and electrode spacing. The Au thickness was held constant at 15 nm, and no Ti was included. Electrode spacing, s, was swept from 5 to 35 nm in increments of 5 nm. For each value of s, the width of the Au structure was swept from 50 to 650 nm in increments of 10 nm. The resulting average optical enhancement values are plotted versus electrode width for three s values in Fig. 3(a). The plot in Fig. 3(b) shows that as electrode spacing decreases for a constant w, average optical enhancement increases nearly exponentially. This is due to plasmonic gap hotspots[54] that increase in field intensity with decreasing s. At each value of s, the peak average enhancement was found at approximately $w = 160$ nm for a constant thickness of $t_{Au} = 15$ nm. At the optimal width and electrode spacing, the enhancement was nearly 25 times greater than for geometries with electrode spacing larger than 15 nm and electrodes larger than 500 nm.

An interesting phenomenon is observed in Fig. 3(a). As Au width is varied, multiple local optical enhancement peaks are observed, and each successive peak decreases in amplitude for increasing w. As w approaches 650 nm, the peaks flatten out. These peaks correspond to specific plasmonic resonant frequencies that couple to the incident light wavelength.[48] These widths are "in tune" with the incident light frequency. Multiple widths exhibit strong plasmonic resonances, indicated by the presence of multiple peaks for each electrode spacing width, but the shortest width demonstrates the strongest peak. The peaks decrease as w increases because plasmons decay as they propagate over longer distances (electrode widths in this case). This is due to damping caused by the oscillating charges colliding with Au atoms, generating heat in the Au. Therefore, the ideal width for maximum enhancement occurs at the smallest w value exhibiting a peak in Fig. 3(a). Another interesting result is that the optical enhancement depends simultaneously on both s and w; however, since the peaks do not shift with s in Fig. 3(a), this indicates that the enhancement is not highly dependent on the specific value of the period, $P = w + s$. Rather, it is maximized when a specific resonant width w is combined with a small value for s.

The optical enhancement was also studied as a function of Au thickness. With w held constant at 160 nm, s held constant at 5 nm, and no Ti layer present in the model, a sweep of Au thickness was conducted from 5 to 60 nm; two values are shown in the enhancement

distributions in Fig. 4. As t_{Au} was increased in this range, the optical enhancement in the GaAs layer increased.

Next, the electrode width w was swept from 10 to 500 nm in 10-nm increments with a 5-nm electrode spacing while also varying the Au thickness. Figure 5 shows that as the

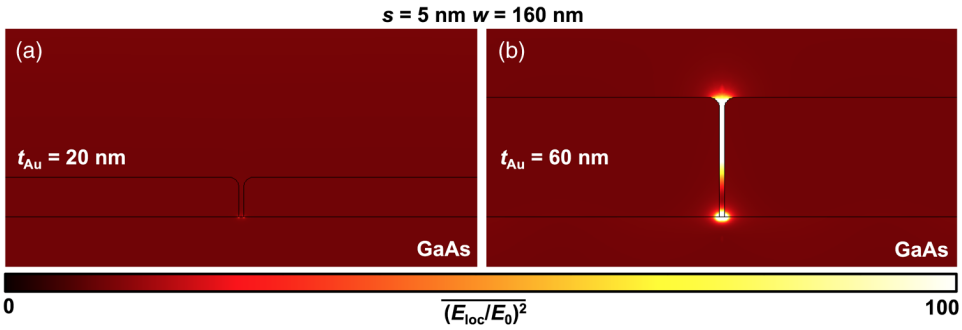

Fig. 4 Calculated optical enhancement distributions for an Au layer in direct contact with a GaAs substrate. The electrode gap was held constant at $s = 5$ nm and the Au width at $w = 160$ nm, where (a) Au thickness $t_{Au} = 20$ nm and (b) $t_{Au} = 60$ nm.

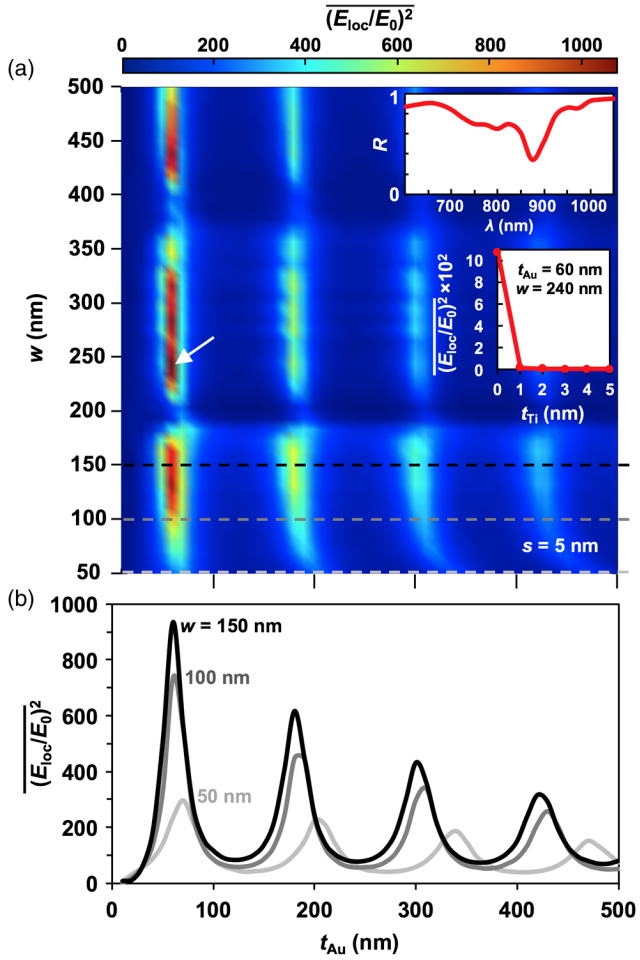

Fig. 5 Effects of Au width (w) and thickness (t_{Au}) on optical enhancement over the entire GaAs layer with no Ti layer included. (a) Color plot showing the average optical enhancement $(E_{loc}/E_0)^2$ as a function of w and t_{Au}. The top inset plots the reflectivity of the structure at the w and t_{Au} values (240 and 60 nm) corresponding to the peak combination shown by the white arrow. The bottom inset plots the enhancement for this specific geometry versus t_{Ti}. (b) Plot of the data along the three dashed lines of constant w shown in (a) $w = 50$, 100, and 150 nm.

w is increased, enhancement peaks occur at specific widths, just as in Fig. 3. Figure 5(a) is a color map of average optical enhancement within the GaAs layer for a range of w and t_{Au} combinations. Figure 5(b) is a plot of the same average enhancement values versus t_{Au} taken at the three constant w values (50, 100, and 150 nm) corresponding to the dashed lines in 5(a). In both Figs. 5(a) and 5(b), local peaks and steady troughs in enhancement can also be seen for increasing t_{Au}. These are also optimal values for t_{Au} that improve the enhancement due to these specific Au thicknesses resonating with plasmons propagating along the vertical wall edge of the structure.[55] The maximum average enhancement occurs when $t_{Au} = 60$ nm and $w = 240$ nm for an incident wavelength of 875 nm. This data point is shown with a white arrow on Fig. 5(a). The top inset plot of Fig. 5(a) is a calculated reflection spectrum for this optimal geometry, showing a resonance at 875 nm, confirming that this ideal geometry is optimized for the GaAs bandgap. The lower inset displays the enhancement provided by this geometric combination versus t_{Ti}. This demonstrates that the smallest Ti thickness is indeed important for obtaining the optimal enhancement. At this ideal geometry, the enhancement was between 10 and 20 times greater than other nonoptimized geometries, demonstrating the potential significance of proper design and modeling for optimal device fabrication.

4 Conclusions

Computational finite element electromagnetic simulations were utilized to analyze the average optical enhancement caused by plasmonic effects of varying geometrical parameters of Au nanostructures on a GaAs semiconductor substrate. It was found that if a layer of Ti is present between the Au and the GaAs layers, optical enhancement in the GaAs is drastically reduced and that the optimal Ti thickness was the smallest value simulated, 1 nm. Effects of the thickness t_{Au}, width w, and electrode spacing s of the Au structures on the optical enhancement were also studied. A significant finding of this work was that, for these structures, the enhancement is not greatly dependent on the period; instead, it depends significantly on the values of w and s. The enhancement is up to 25 times stronger than for nonideal geometries when a highly resonant Au width is combined with a small gap between structures. Optimal dimensions of the structure in this configuration were found to be $w = 240$ nm, $t_{Au} = 60$ nm, and $s = 5$ nm. Also interesting was the result that the optimal w increases as t_{Au} increases. For the smaller thickness of 15 nm, the optimal width was 160 nm. This is important to consider when working with different device thickness. For larger thicknesses, the most strongly resonant plasmonic mode is supported by larger Au widths. Decreasing the thickness requires a lower width to optimally support this strongest resonant mode. Additional enhancement peaks were also observed over a range of widths and thicknesses corresponding to the plasmonic resonance frequencies and the incident light wavelength.[48]

Overall, the enhancement value $(E_{loc}/E_0)^2$ increases from ~3 at a large interelectrode spacing of 35 nm to around 1100 for an optimized geometry. This is more than a 300 times increase in the optical enhancement in the GaAs layer. This could improve the device efficiency of a hypothetical photodetector, for instance, by 1 to 2 orders of magnitude. It is likely that improvements in the device efficiency will be less than 300 times greater in an actual device due to recombination losses and the precise current densities within the GaAs. Future work is needed to determine this exact efficiency increase.

Acknowledgments

Funding has been provided by the National Science Foundation Grant Award Nos. 1460754 and 359306. We would also like to acknowledge financial support from the Arkansas Biosciences Institute, the major research component of the Arkansas Tobacco Settlement Proceeds Act of 2000. Ahmad Darweesh was supported by the Iraqi Ministry of Higher Education and Scientific Research, and Stephen J. Bauman was supported by the Doctoral Academy Fellowship through the University of Arkansas Graduate School as well as the SPIE Optics and Photonics Education Scholarship.

References

1. E. Ozbay, "Plasmonics: merging photonics and electronics at nanoscale dimensions," *Science* **311**(5758), 189–193 (2006).
2. C. Saylor et al., "Investigation of maximum optical enhancement in single gold nanowires and triple nanowire arrays," *J. Nanophotonics* **9**(1), 093053 (2015).
3. N. Burford and M. El-Shenawee, "Optimization of silver nanotoroid arrays for the absorption enhancement of silicon thin-film solar cells," *Plasmonics* **10**(1), 225–232 (2015).
4. S. A. Maier, *Plasmonics: Fundamentals and Applications*, Springer, New York (2007).
5. K.-L. Lee et al., "Sensitive biosensor array using surface plasmon resonance on metallic nanoslits," *J. Biomed. Opt.* **12**(4), 044023 (2007).
6. Y. S. Jung et al., "Blue-shift of surface plasmon resonance in a metal nanoslit array structure," *Opt. Express* **17**(18), 16081 (2009).
7. C. L. Tan et al., "Absorption enhancement of 980 nm MSM photodetector with a plasmonic grating structure," *Opt. Commun.* **283**(9), 1763–1767 (2010).
8. M. Grande et al., "Asymmetric plasmonic grating for optical sensing of thin layers of organic materials," *Sens. Actuators B Chem.* **160**(1), 1056–1062 (2011).
9. M. Shalaby et al., "Concurrent field enhancement and high transmission of THz radiation in nanoslit arrays," *Appl. Phys. Lett.* **99**(4), 041110 (2011).
10. N. Livneh et al., "Highly directional emission and photon beaming from nanocrystal quantum dots embedded in metallic nanoslit arrays," *Nano Lett.* **11**(4), 1630–1635 (2011).
11. K.-L. Lee et al., "Enhancing surface plasmon detection using template-stripped gold nanoslit arrays on plastic films," *ACS Nano* **6**(4), 2931–2939 (2012).
12. Y. Gao, Q. Gan, and F. J. Bartoli, "Spatially selective plasmonic sensing using metallic nanoslit arrays," *IEEE J. Sel. Top. Quantum Electron.* **20**(3), 96–101 (2014).
13. A. A. Darweesh, S. J. Bauman, and J. B. Herzog, "Improved optical enhancement using double-width plasmonic gratings with nanogaps," *Photonics Res.* **4**(5), 173–180 (2016).
14. K.-L. Lee, W.-S. Wang, and P.-K. Wei, "Sensitive label-free biosensors by using gap plasmons in gold nanoslits," *Biosens. Bioelectron.* **24**(2), 210–215 (2008).
15. L. Verslegers et al., "Planar lenses based on nanoscale slit arrays in a metallic film," *Nano Lett.* **9**(1), 235–238 (2009).
16. A. E. Çetin, K. Güven, and Ö. E. Müstecaplıoğlu, "Active control of focal length and beam deflection in a metallic nanoslit array lens with multiple sources," *Opt. Lett.* **35**(12), 1980–1982 (2010).
17. T. Tanemura et al., "Multiple-wavelength focusing of surface plasmons with a nonperiodic nanoslit coupler," *Nano Lett.* **11**(7), 2693–2698 (2011).
18. K. Iwami et al., "Ultrasmall radial polarizer array based on patterned plasmonic nanoslits," *Appl. Phys. Lett.* **101**(16), 161119 (2012).
19. W. Zhu et al., "Lithographically fabricated optical antennas with gaps well below 10 nm," *Small* **7**(13), 1761–1766 (2011).
20. X. Chen et al., "Atomic layer lithography of wafer-scale nanogap arrays for extreme confinement of electromagnetic waves," *Nat. Commun.* **4**, 2361 (2013).
21. X. Chen et al., "Nanogap-enhanced infrared spectroscopy with template-stripped wafer-scale arrays of buried plasmonic cavities," *Nano Lett.* **15**(1), 107–113 (2015).
22. C. Lumdee, B. Yun, and P. G. Kik, "Gap-plasmon enhanced gold nanoparticle photoluminescence," *ACS Photonics* **1**(11), 1224–1230 (2014).
23. J. B. Herzog et al., "Dark plasmons in hot spot generation and polarization in interelectrode nanoscale junctions," *Nano Lett.* **13**(3), 1359–1364 (2013).
24. A. De Leebeeck et al., "On-chip surface-based detection with nanohole arrays," *Anal. Chem.* **79**(11), 4094–4100 (2007).
25. R. Gordon et al., "Plasmonic sensors based on nano-holes: technology and integration," *Proc. SPIE* **6959**, 695913 (2008).
26. F. Eftekhari et al., "Nanoholes as nanochannels: flow-through plasmonic sensing," *Anal. Chem.* **81**(11), 4308–4311 (2009).
27. M. D. Sonntag et al., "Molecular plasmonics for nanoscale spectroscopy," *Chem. Soc. Rev.* **43**(4), 1230–1247 (2014).

28. K. R. Catchpole and A. Polman, "Plasmonic solar cells," *Opt. Express* **16**(26), 21793 (2008).
29. K. Nakayama, K. Tanabe, and H. A. Atwater, "Plasmonic nanoparticle enhanced light absorption in GaAs solar cells," *Appl. Phys. Lett.* **93**(12), 121904 (2008).
30. H. A. Atwater and A. Polman, "Plasmonics for improved photovoltaic devices," *Nat. Mater.* **9**(3), 205–213 (2010).
31. V. E. Ferry et al., "Light trapping in ultrathin plasmonic solar cells," *Opt. Express* **18**(S2), A237–A245 (2010).
32. A. Aubry et al., "Plasmonic light-harvesting devices over the whole visible spectrum," *Nano Lett.* **10**(7), 2574–2579 (2010).
33. I. Thomann et al., "Plasmon enhanced solar-to-fuel energy conversion," *Nano Lett.* **11**(8), 3440–3446 (2011).
34. J. N. Munday and H. A. Atwater, "Large integrated absorption enhancement in plasmonic solar cells by combining metallic gratings and antireflection coatings," *Nano Lett.* **11**(6), 2195–2201 (2011).
35. R. Yu et al., "Nanomaterials and nanostructures for efficient light absorption and photovoltaics," *Nano Energy* **1**(1), 57–72 (2012).
36. G. Raschke et al., "Biomolecular recognition based on single gold nanoparticle light scattering," *Nano Lett.* **3**(7), 935–938 (2003).
37. J. Homola, "Present and future of surface plasmon resonance biosensors," *Anal. Bioanal. Chem.* **377**(3), 528–539 (2003).
38. P. K. Jain et al., "Review of some interesting surface plasmon resonance-enhanced properties of noble metal nanoparticles and their applications to biosystems," *Plasmonics* **2**(3), 107–118 (2007).
39. J. N. Anker et al., "Biosensing with plasmonic nanosensors," *Nat. Mater.* **7**(6), 442–453 (2008).
40. T. Chung et al., "Plasmonic nanostructures for nano-scale bio-sensing," *Sensors* **11**(11), 10907 (2011).
41. A. G. Brolo, "Plasmonics for future biosensors," *Nat. Photonics* **6**(11), 709–713 (2012).
42. A. Sivanesan et al., "Reproducible and label-free biosensor for the selective extraction and rapid detection of proteins in biological fluids," *J. Nanobiotechnol.* **13**(1), 43 (2015).
43. N. Das et al., "Analysis of nano-grating-assisted light absorption enhancement in metal–semiconductor–metal photodetectors patterned using focused ion-beam lithography," *Opt. Commun.* **284**(6), 1694–1700 (2011).
44. A. Karar et al., "High-responsivity plasmonics-based GaAs metal-semiconductor-metal photodetectors," *Appl. Phys. Lett.* **99**(13), 133112 (2011).
45. A. I. Nusir et al., "Near-infrared metal-semiconductor-metal photodetector based on semi-insulating GaAs and interdigital electrodes," *Photonics Res.* **3**(1), 1–4 (2015).
46. A. M. Hill et al., "Computational electromagnetic study of plasmonic effects in interdigital arrays," *Proc. SPIE* **9163**, 91633Q (2014).
47. S. J. Bauman et al., "Fabrication of sub-lithography-limited structures via nanomasking technique for plasmonic enhancement applications," *IEEE Trans. Nanotechnol.* **14**(5), 790–793 (2015).
48. A. A. Darweesh et al., "Improved optical enhancement in binary plasmonic gratings with nanogap spacing," *Proc. SPIE* **9927**, 99270Z (2016).
49. T. Siegfried et al., "Engineering metal adhesion layers that do not deteriorate plasmon resonances," *ACS Nano* **7**(3), 2751–2757 (2013).
50. P. B. Johnson and R. W. Christy, "Optical constants of the noble metals," *Phys. Rev. B* **6**(12), 4370–4379 (1972).
51. E. D. Palik, *Handbook of Optical Constants of Solids*, Academic Press, San Diego (1998).
52. G. P. Abbey et al., "Structural characteristics of Au-GaAs nanostructures for increased plasmonic optical enhancement," *Proc. SPIE* **9758**, 97580N (2016).
53. D. T. Debu et al., "Surface plasmon damping effects due to Ti adhesion layer in individual gold nanodisks," *Opt. Mater. Express* **7**(1), 73–84 (2017).

54. D. Natelson, Y. Li, and J. B. Herzog, "Nanogap structures: combining enhanced Raman spectroscopy and electronic transport," *Phys. Chem. Chem. Phys.* **15**(15), 5262–5275 (2013).
55. A. Sobhani et al., "Narrowband photodetection in the near-infrared with a plasmon-induced hot electron device," *Nat. Commun.* **4**, 1643 (2013).

Zachary T. Brawley is an undergraduate physics major at the University of Central Arkansas. He will graduate in 2017 and intends to pursue a PhD as a graduate student focusing on plasmonic/material science research.

Stephen J. Bauman is a PhD candidate of the microelectronics and photonics graduate program at the University of Arkansas. He received his MS degree in microelectronics and photonics from the University of Arkansas in 2015 and his BS degree in physics and engineering physics from Southeast Missouri State University in 2013. He is an active student member of SPIE and is a cofounder and the current president of the Arkansas Laserbacks student chapter.

Grant P. Abbey currently works for Texas Instruments. He received his BS degree from Mississippi State University in 2016, and he was an REU student in the Herzog Lab in the summer of 2015.

Ahmad A. Darweesh is working on his PhD in the microelectronics-photonics graduate program at the University of Arkansas. He received his MS degree from Al-Mustansiriyah University in Baghdad, Iraq. He is a student member of SPIE and currently an officer of the Arkansas Laserbacks student chapter.

Ahmad I. Nusir received his BS degree in electrical engineering from the University of Jordan, Amman, and his MS degree in electrical engineering from the University of Arkansas, Fayetteville. Currently, he is a PhD candidate in the Electrical Engineering Department at the University of Arkansas. Since 2012, he has worked in the Optoelectronics Research Lab at the University of Arkansas. His current research is focused on microelectronics, nanofabrication, photonics, and photovoltaics.

Omar Manasreh is a professor in the Department of Electrical Engineering at the University of Arkansas. He received his PhD from the University of Arkansas. He has extensive experience in experimental and theoretical optoelectronic properties of III–V semiconductors, superlattices, nanostructures, and related devices. He is a senior member of IEEE.

Joseph B. Herzog is an assistant professor in the Department of Physics at the University of Arkansas. He received his BS degree from Louisiana State University and his MS degree and PhD from the University of Notre Dame. He was a postdoctoral research associate at Rice University before joining the University of Arkansas. His research focuses on nano-optics, including plasmonics and photonic crystals. He is an active member of SPIE, serving on various committees.